

Modified Low Temperature Solution Combustion Synthesis and Electrochemical Properties of $\text{Li}_{1-x}\text{Na}_x\text{Ni}_{0.5}\text{Mn}_{1.5}\text{O}_4$ ($x=0.05, 0.10$) Materials as Cathode for Lithium-Ion Batteries

Hongyan Sun^{1,2}, Xin Kong^{1,2}, Baosen Wang^{1,2}, Shaoping Feng^{1,2}, Guiyang Liu^{1,2,*}

¹ Department of Chemistry, College of Science, Honghe University, Mengzi, 661199, Yunnan, China

² Local Characteristic Resource Utilization and New Materials Key Laboratory of Universities in Yunnan, Honghe University, Mengzi 661199, Yunnan, China.

*E-mail: liuguiyang@tsinghua.org.cn

Received: 13 August 2018 / Accepted: 10 October 2018 / Published: 30 November 2018

The $\text{Li}_{0.95}\text{Na}_{0.05}\text{Ni}_{0.5}\text{Mn}_{1.5}\text{O}_4$ and $\text{Li}_{0.90}\text{Na}_{0.10}\text{Ni}_{0.5}\text{Mn}_{1.5}\text{O}_4$ cathode materials were first synthesized by a modified low temperature solution combustion synthesis method. XRD and SEM are used to characterize the phase structure and micro morphologies of samples. The results show that the main crystal phase is $\text{LiNi}_{0.5}\text{Mn}_{1.5}\text{O}_4$ with traces of secondary phase of $\text{Na}_{0.70}\text{MnO}_2$ for both samples. And the impurity phase increases with the increasing of Na doping content. Meanwhile, both samples exhibit perfect octahedral spinel structure. The electrochemical properties are studied by galvanostatic charge-discharge testing, cyclic voltammetry (CV) and electrochemical impedance spectroscopy (EIS) techniques in detail. The electrochemical performances results indicate that the initial coulomb efficiencies of the $\text{Li}_{0.95}\text{Na}_{0.05}\text{Ni}_{0.5}\text{Mn}_{1.5}\text{O}_4$ and $\text{Li}_{0.90}\text{Na}_{0.10}\text{Ni}_{0.5}\text{Mn}_{1.5}\text{O}_4$ are 89.2% and 84%, respectively. The two samples both deliver remarkable capacity retention approximately 91.0% after 500 cycles at 1C rate at 25 °C. The capacity retention of $\text{Li}_{0.95}\text{Na}_{0.05}\text{Ni}_{0.5}\text{Mn}_{1.5}\text{O}_4$ sample is 96.5% after 100 cycles at 10C rate, and can still deliver a specific capacity of more than 110mAh/g, indicating that it is a promising cathode material for Li-ion batteries.

Keywords: $\text{LiNi}_{0.5}\text{Mn}_{1.5}\text{O}_4$, Lithium ion batteries, Na doping, Electrochemical performance

1. INTRODUCTION

Due to high capacity, high rate capability, superior safety, and long life, lithium ion battery has been applied in electric vehicles (EVs) and hybrid electric vehicles (HEVs) industries [1-4]. It is well known that the working voltage and power density is mainly determined by the performance of the cathode materials [5]. Among the many cathode materials, $\text{LiNi}_{0.5}\text{Mn}_{1.5}\text{O}_4$ (LNMO) has attracted

intensive attention because that it has higher operating voltage, energy density and power density[6,7]. Unfortunately, it is reported that the cycling stability of LNMO at high rate is not satisfactory, especially at elevated temperatures[8]. To solve these problems, many efforts have been made by researchers on synthesis method, surface coating, doping, and so on. According to relevant reports, cations doping is considered as an effective technique to improve the electrochemical performance of LNMO[9-12]. As far as we know, Na-doping at Li site can effectively improve the rate capability of LNMO reported by other groups[13,14]. The $\text{Li}_{1-x}\text{Na}_x\text{Ni}_{0.5}\text{Mn}_{1.5}\text{O}_4$ doping with 1%, 3%, 5% and 10%Na are prepared by Wang et al. with a co-precipitation method followed by a solid-state method. The research results are shown that the proper Na doping can enhance the cycling performance and rate capacity greatly. The capacity retention is 93% after 100 cycles at 1C at 25°C and with a discharge specific capacity of 101.3 mAh/g at 10C for the sample with the Na doping content of 5%. However, the $\text{Li}_{0.95}\text{Na}_{0.05}\text{Ni}_{0.5}\text{Mn}_{1.5}\text{O}_4$ synthesized by Wang et al. with a simple solid-state method is reported that the Na doping can only improve the rate capacity effectively, but not the cycling stability.

Encouraged by the two groups' research results, in the paper we have prepared $\text{Li}_{1-x}\text{Na}_x\text{Ni}_{0.5}\text{Mn}_{1.5}\text{O}_4$ ($x=0.05, 0.10$) cathode materials by modified low temperature solution combustion synthesis method, which was not reported at elsewhere.

2. EXPERIMENTAL

The $\text{Li}_{1-x}\text{Na}_x\text{Ni}_{0.5}\text{Mn}_{1.5}\text{O}_4$ ($x=0.05, 0.10$) samples were prepared via the modified low temperature solution combustion synthesis method. The LiNO_3 , CH_3COOLi , $\text{Ni}(\text{NO}_3)_2$, $(\text{CH}_3\text{COO})_2\text{Ni}$, $\text{Mn}(\text{NO}_3)_2$, $(\text{CH}_3\text{COO})_2\text{Mn}$ and NaNO_3 were working as starting materials. At the same time, the mole ratio between nitrate and acetate for Li, Ni and Mn ions was set to 1:1. The details of synthesis process were reported in our previous researches[15-18].

Powder XRD (PANalytical X'pert pro, Cu-K α radiation) was employed to characterize the phase structure of $\text{Li}_{0.95}\text{Na}_{0.05}\text{Ni}_{0.5}\text{Mn}_{1.5}\text{O}_4$ and $\text{Li}_{0.90}\text{Na}_{0.10}\text{Ni}_{0.5}\text{Mn}_{1.5}\text{O}_4$ samples. The morphologies of products were observed using the field emission scanning electron microscopy(SEM, FEI Quanta FEG 250).

The electrochemical performance was evaluated with CR2025-type coin cells. The detailed preparation flow of positive electrodes and coin cells were described in our other studies[16,18]. Cells were galvanostatically charged and discharged on a battery test system(LANHE CT2001A instrument, Wuhan, China) at room temperature in the voltage range of 3.5-5.0V at different C rates(1C=150mA/g). Cyclic voltammogram(CV) and electrochemical impedance spectroscopy (EIS) of the cells were measured using an electrochemical workstation(CHI 660). The scan rate was from 0.1 to 0.5mV/s with a voltage range of 3.5-5.0V. The frequency range was from 100 kHz to 0.1 Hz with an AC amplitude voltage of 5mV.

3. RESULTS AND DISCUSSION

3.1 Phase structure

The XRD patterns of samples are shown in Fig. 1. The results reveal that the main crystal phase is $\text{LiNi}_{0.5}\text{Mn}_{1.5}\text{O}_4$ for both samples, and with traces of secondary phase of $\text{Na}_{0.70}\text{MnO}_2$ (27-0752). In

addition, the diffraction intensity of impurity phase increases with the increase of Na addition content, indicating that the doped Na can not fully enter the lattice and some impurities generate when relatively high concentration of Na doping.

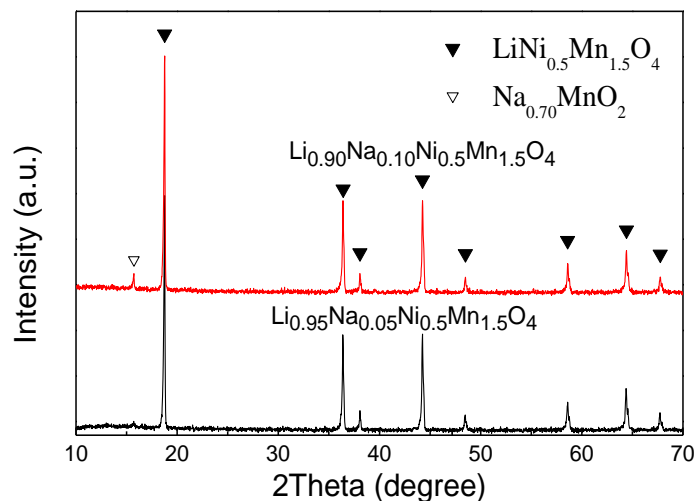


Figure 1. XRD patterns of the samples

3.2 Morphology

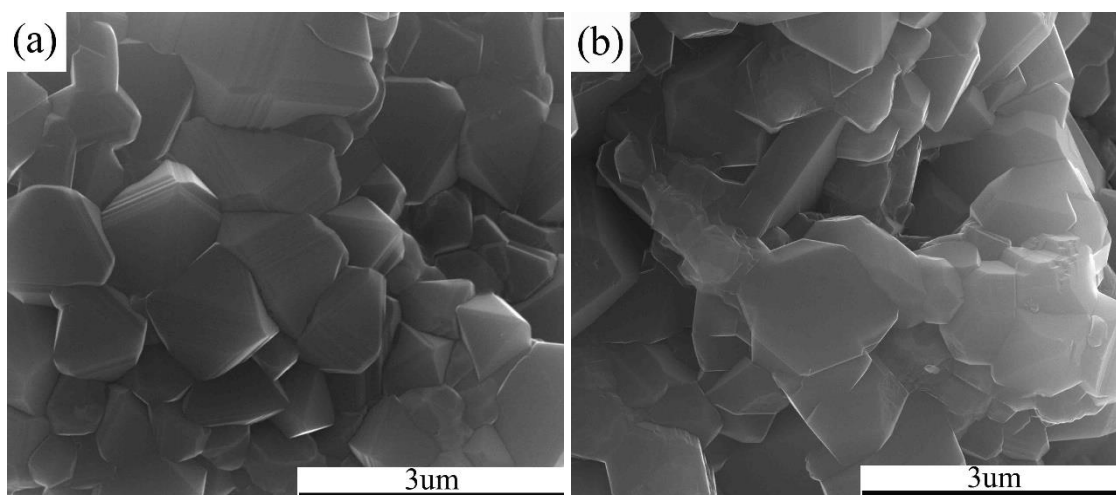


Figure 2. SEM micro morphologies of the samples (a) $\text{Li}_{0.95}\text{Na}_{0.05}\text{Ni}_{0.5}\text{Mn}_{1.5}\text{O}_4$, (b) $\text{Li}_{0.90}\text{Na}_{0.10}\text{Ni}_{0.5}\text{Mn}_{1.5}\text{O}_4$

Fig. 2 shows the SEM micro morphologies of the samples. As shown, both samples exhibit a perfect octahedral spinel structure. However, the particles of $\text{Li}_{0.95}\text{Na}_{0.05}\text{Ni}_{0.5}\text{Mn}_{1.5}\text{O}_4$ are more homogeneous and better development than those of $\text{Li}_{0.90}\text{Na}_{0.10}\text{Ni}_{0.5}\text{Mn}_{1.5}\text{O}_4$.

3.3 Electrochemical performance

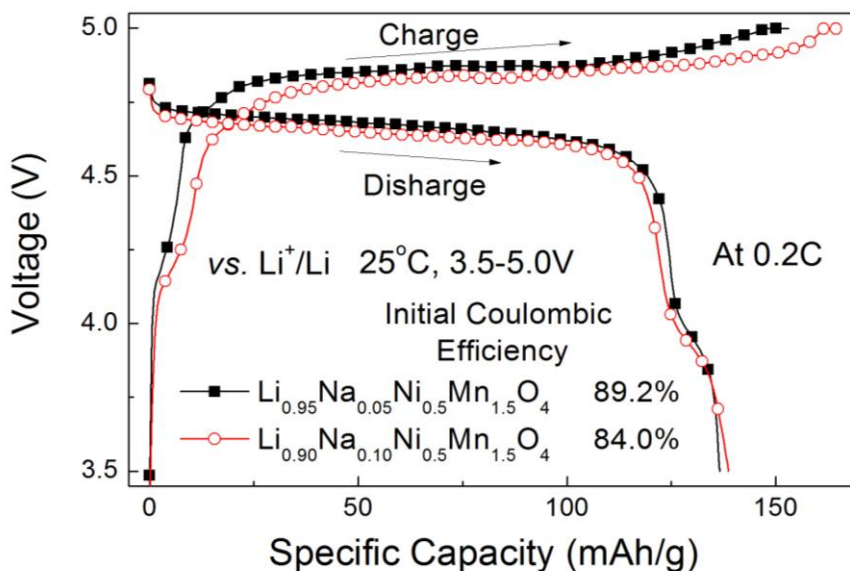


Figure 3. Initial charge/discharge curves for the samples at 0.2C and at 25°C

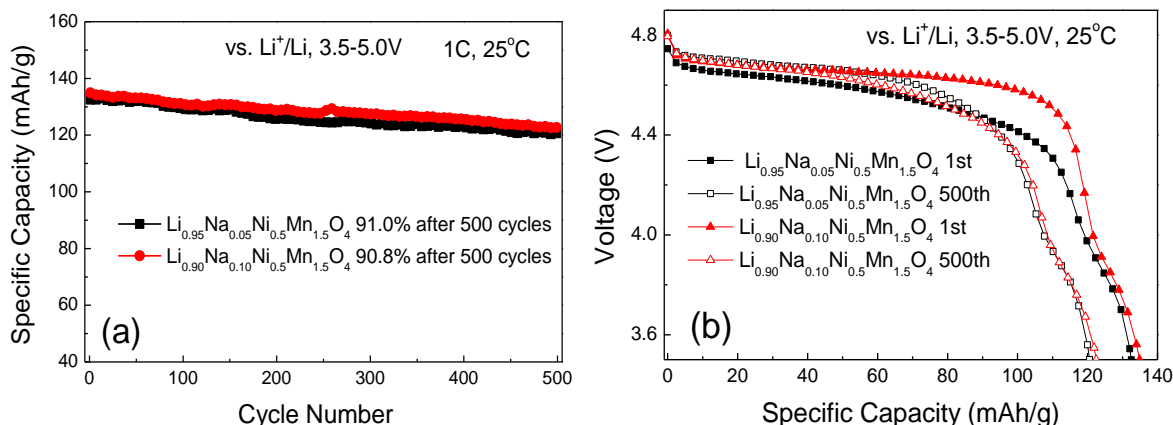


Figure 4. (a) Cycling performance and (b) the discharge curves of the first and the 500th cycles at 1C rate of the samples at 25°C

Fig. 3 illustrates the initial charge/discharge curves for the samples at 0.2C and 25°C. Obviously there are two voltage plateaus at around 4.7V(main) and 4.0V(minor) regions which corresponding to Ni^{2+/4+} and Mn^{3+/4+} redox couples in two samples, suggesting that the two samples have a combination structure of ordered P4₃32 space group and disordered Fd-3m space group[19]. Moreover, the initial coulomb efficiencies of the Li_{0.95}Na_{0.05}Ni_{0.5}Mn_{1.5}O₄ and Li_{0.90}Na_{0.10}Ni_{0.5}Mn_{1.5}O₄ are 89.2% and 84%, respectively. Noticeably, the Li_{0.95}Na_{0.05}Ni_{0.5}Mn_{1.5}O₄ sample has a higher initial charge and discharge efficiency than that of Li_{0.90}Na_{0.10}Ni_{0.5}Mn_{1.5}O₄.

The cycling performance and the discharge curves of the first and the 500th cycles of the samples at 1C rate at 25°C are given in Fig. 4. From Fig. 4(a), it can be seen that the two samples both deliver

remarkable capacity retention of 91.0% and 90.8% for $\text{Li}_{0.95}\text{Na}_{0.05}\text{Ni}_{0.5}\text{Mn}_{1.5}\text{O}_4$ and $\text{Li}_{0.90}\text{Na}_{0.10}\text{Ni}_{0.5}\text{Mn}_{1.5}\text{O}_4$ after 500 cycles, respectively. The results indicate that the cyclic performance of LNMO at room temperature can be improved by Na-doping. As shown in Fig. 4(b), the voltage platforms don't suffer an obvious attenuation for both samples. On the contrary, the voltage platform of the $\text{Li}_{0.95}\text{Na}_{0.05}\text{Ni}_{0.5}\text{Mn}_{1.5}\text{O}_4$ sample has a slightly increase.

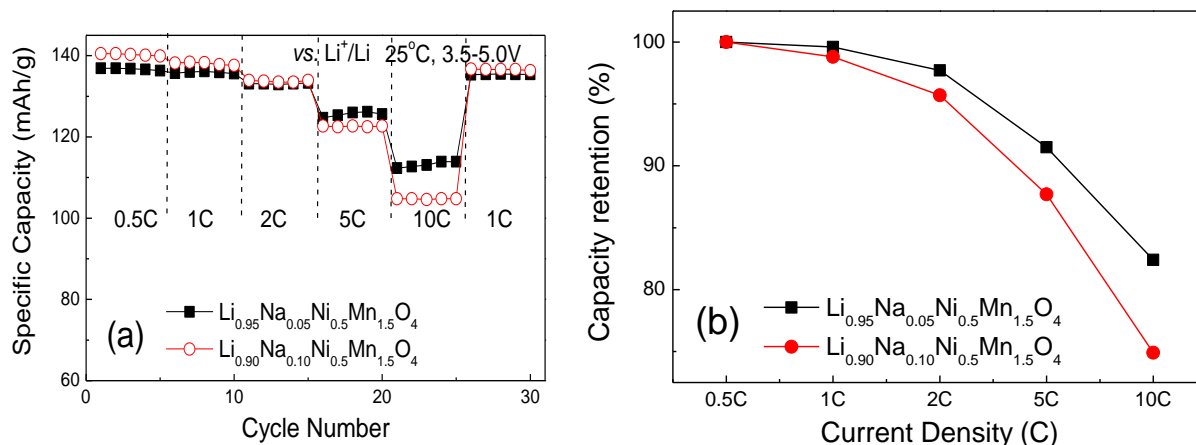


Figure 5. (a) Rate capabilities (b) capacity retentions at different rates of the samples at room temperature.

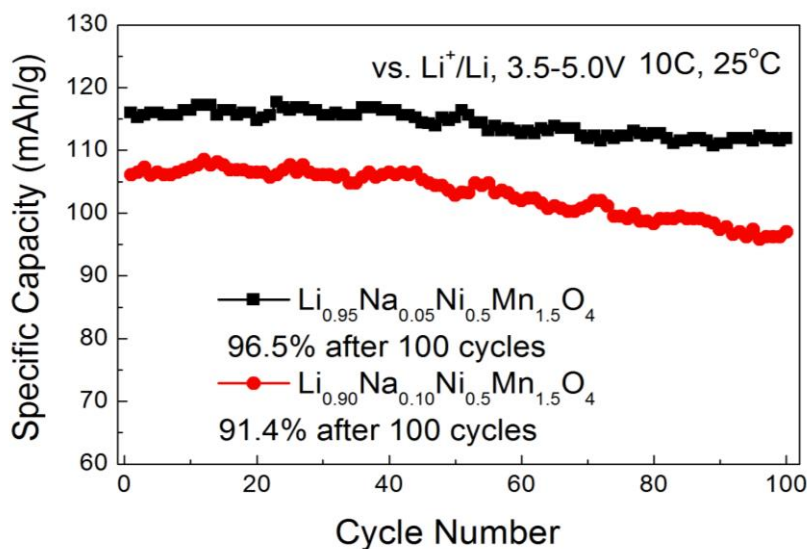


Figure 6. Cycling performance of the samples at 10C rate (Charged at 0.5C, and discharged at 10C)

The rate capability is one of the most important properties for the positive electrode during the practical commercial application for the electric vehicles (EVs) or hybrid electric vehicles (HEVs). Fig. 5 compares the rate capabilities and capacity retentions of the $\text{Li}_{0.95}\text{Na}_{0.05}\text{Ni}_{0.5}\text{Mn}_{1.5}\text{O}_4$ and the $\text{Li}_{0.90}\text{Na}_{0.10}\text{Ni}_{0.5}\text{Mn}_{1.5}\text{O}_4$ samples at different rates. It is clearly observed that the capacities of the two samples decrease with increasing discharge rate due to electrode polarization. However, the $\text{Li}_{0.95}\text{Na}_{0.05}\text{Ni}_{0.5}\text{Mn}_{1.5}\text{O}_4$ sample has a better rate capability than the other one. The improved rate

capabilities may be possibly attributed to that the $\text{Li}_{0.95}\text{Na}_{0.05}\text{Ni}_{0.5}\text{Mn}_{1.5}\text{O}_4$ sample has purer crystal phase and better crystal development which shown in Fig. 1 and Fig. 2. And the $\text{Li}_{0.95}\text{Na}_{0.05}\text{Ni}_{0.5}\text{Mn}_{1.5}\text{O}_4$ sample can still deliver a specific capacity of more than 110mAh/g at 10C rate, which is higher than the 5% Na-LNMO prepared by Wang et al.[14]. Moreover, the capacity retention of the $\text{Li}_{0.95}\text{Na}_{0.05}\text{Ni}_{0.5}\text{Mn}_{1.5}\text{O}_4$ sample can reach 82.4% at 10C rate, which is higher than $\text{Li}_{0.95}\text{Ni}_{0.45}\text{Mn}_{0.5}\text{Al}_{0.05}\text{O}_4$ reported by Zhong et al.[20]

As far as we know, the cyclic stability at fast discharge condition is very important during the practical commercial application for the electric vehicles(EVs) and hybrid electric vehicles(HEVs). The cycling performance of samples at 10C rate is given in Fig. 6. It is apparent that the $\text{Li}_{0.95}\text{Na}_{0.05}\text{Ni}_{0.5}\text{Mn}_{1.5}\text{O}_4$ sample has more excellent cycle performance at high rate. The capacity retention of $\text{Li}_{0.95}\text{Na}_{0.05}\text{Ni}_{0.5}\text{Mn}_{1.5}\text{O}_4$ sample is 96.5% after 100 cycles at 10C rate. On the other hand, the $\text{Li}_{0.90}\text{Na}_{0.10}\text{Ni}_{0.5}\text{Mn}_{1.5}\text{O}_4$ can only retain 91.4% at the same operation condition, exhibiting poor cycle stability at high rate.

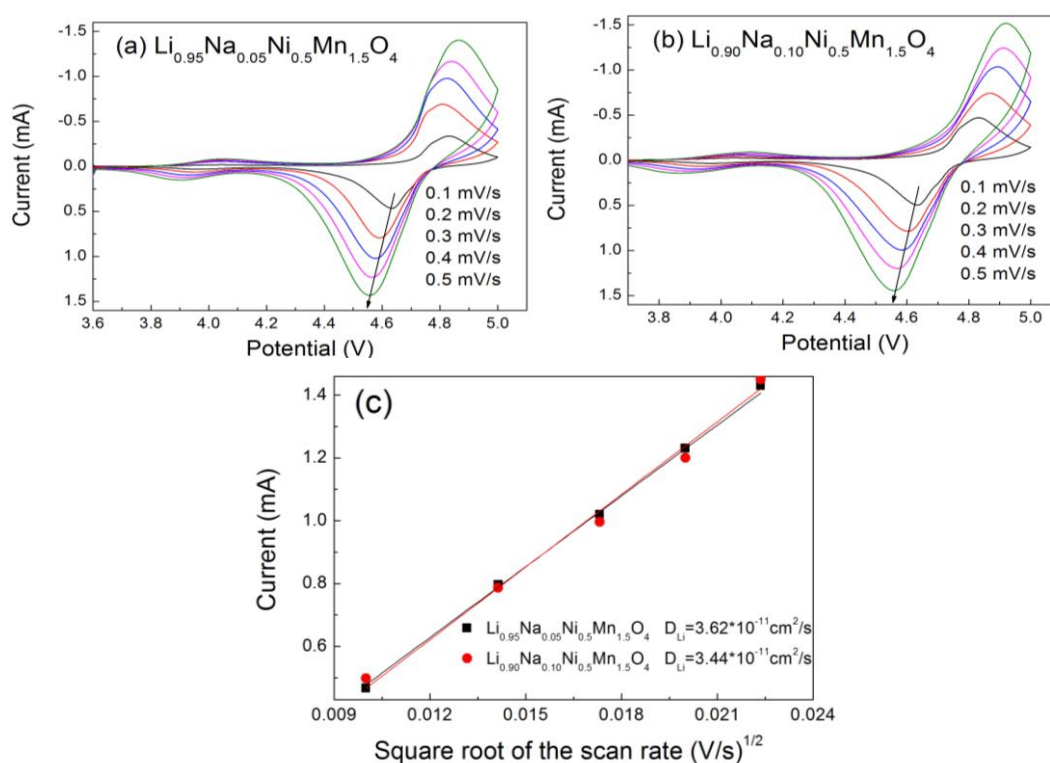


Figure 7. Cyclic voltammograms (CVs) of (a) $\text{Li}_{0.95}\text{Na}_{0.05}\text{Ni}_{0.5}\text{Mn}_{1.5}\text{O}_4$ and (b) $\text{Li}_{0.90}\text{Na}_{0.10}\text{Ni}_{0.5}\text{Mn}_{1.5}\text{O}_4$ at different scan rates. (c) The plotting of peak current vs. square root of the scan rate for the two samples.

In order to better understand the reason for the excellent electrochemical performance of the samples, we perform a series of CV tests for the two samples. Fig. 7(a) and Fig. 7(b) show the CV curves of the two samples at the scanning rate from 0.10mV/s to 0.50mV/s. It can be seen that the two samples both possess a sharp oxidation/reduction peak of $\text{Ni}^{2+}/\text{Ni}^{4+}$ at 4.7V and a very small oxidation/reduction peak of $\text{Mn}^{3+}/\text{Mn}^{4+}$ at 4.0V. The result indicates that the products have a very high degree of ordering, which is well consistent with the discharge curves result above. Meanwhile, the CV curves of

$\text{Li}_{0.95}\text{Na}_{0.05}\text{Ni}_{0.5}\text{Mn}_{1.5}\text{O}_4$ sample shows less deformation with the increase of scanning speed indicating that it possesses lower polarization and better conductivity.

Lantelme et al. [21] have reported that the peak current is proportional to the square root of the scanning rate, which can be obtained according to CV curves at different scanning rates. And the calculation formula of D_{Li} at room temperature was given by Ref. [22].

$$i_p = 2.69 \times 10^5 n^{\frac{3}{2}} A C_{\text{Li}} D_{\text{Li}}^{\frac{1}{2}} \nu^{\frac{1}{2}}$$

In where, I_p represents the peak current(A), n (for lithium-ion, $n=1$) represents the number of electrons per reaction species, A is surface area of the electrode (2 cm^2 in our study) and C_{Li} (given as 0.02378 mol/cm^3) is the bulk concentration of Li^+ in the electrode.

Fig. 7(c) presents the i_p vs. the square root of the scan rates ($\nu^{1/2}$) of the samples. D_{Li} can be calculated from the slop of i_p vs $\nu^{1/2}$ plots according to the above formula. The D_{Li} of the $\text{Li}_{0.95}\text{Na}_{0.05}\text{Ni}_{0.5}\text{Mn}_{1.5}\text{O}_4$ electrode and $\text{Li}_{0.90}\text{Na}_{0.10}\text{Ni}_{0.5}\text{Mn}_{1.5}\text{O}_4$ electrode are $3.62 \times 10^{-11} \text{ cm}^2/\text{s}$ and $3.44 \times 10^{-11} \text{ cm}^2/\text{s}$, respectively. They are superior to many other $\text{LiNi}_{0.5}\text{Mn}_{1.5}\text{O}_4$ materials reported by other groups [8,9]. The comparison of the D_{Li} with other $\text{LiNi}_{0.5}\text{Mn}_{1.5}\text{O}_4$ materials is summarized in Table 1. As show in Fig. 7(c), the D_{Li} value of the $\text{Li}_{0.95}\text{Na}_{0.05}\text{Ni}_{0.5}\text{Mn}_{1.5}\text{O}_4$ sample is slightly bigger that of the $\text{Li}_{0.90}\text{Na}_{0.10}\text{Ni}_{0.5}\text{Mn}_{1.5}\text{O}_4$ sample, which is favorable for getting better rate capabilities.

Table 1. Comparison of the diffusion coefficient of lithium(D_{Li})

Literatures	Samples	$D_{\text{Li}}/(\text{ cm}^2/\text{s})$
Our research	$\text{Li}_{0.95}\text{Na}_{0.05}\text{Ni}_{0.5}\text{Mn}_{1.5}\text{O}_4$	3.62×10^{-11}
Our research	$\text{Li}_{0.90}\text{Na}_{0.10}\text{Ni}_{0.5}\text{Mn}_{1.5}\text{O}_4$	3.44×10^{-11}
Reference[8]	$\text{LiNi}_{0.525}\text{Mn}_{1.425}\text{Nb}_{0.05}\text{O}_4$	10.07×10^{-16}
Reference[9]	$\text{LiNi}_{0.5}\text{Mn}_{1.4}\text{Mg}_{0.1}\text{O}_4$	5.30×10^{-12}

The electrochemical impedance spectroscopy(EIS) of samples is plotted in Fig. 8, and the possible equivalent circuit is also inserted in Fig. 8. The EIS are measured in the frequency range from 0.1Hz to 100kHz after 3rd cycles. The EIS spectra of two samples display the similar profile, which are combined with a depressed semicircle at high-to-middle frequency region and an inclined line in the low frequency region. In the equivalent circuit, the electrolyte resistance (R_s) is expressed by the intercept at the Z' axis, the charge transfer resistance (R_{ct}) is expressed by the semicircle in high-to-middle frequency region, and the value of lithium-ion migration resistance (R_f) through the multilayer surface films can be determined from the diameter of the semicircle[2, 23]. From Fig. 8, it can be seen that the R_{ct} of two samples are both small indicating that they have low electrochemical polarization, which will lead to higher rate capability. Meanwhile, the slope in the low-frequency region of EIS are both large for two samples, suggesting that the two samples have large D_{Li} [24, 25]. As shown, the R_{ct} of

$\text{Li}_{0.95}\text{Na}_{0.05}\text{Ni}_{0.5}\text{Mn}_{1.5}\text{O}_4$ is smaller than that of $\text{Li}_{0.90}\text{Na}_{0.10}\text{Ni}_{0.5}\text{Mn}_{1.5}\text{O}_4$, and it can lead to higher rate capability performance.

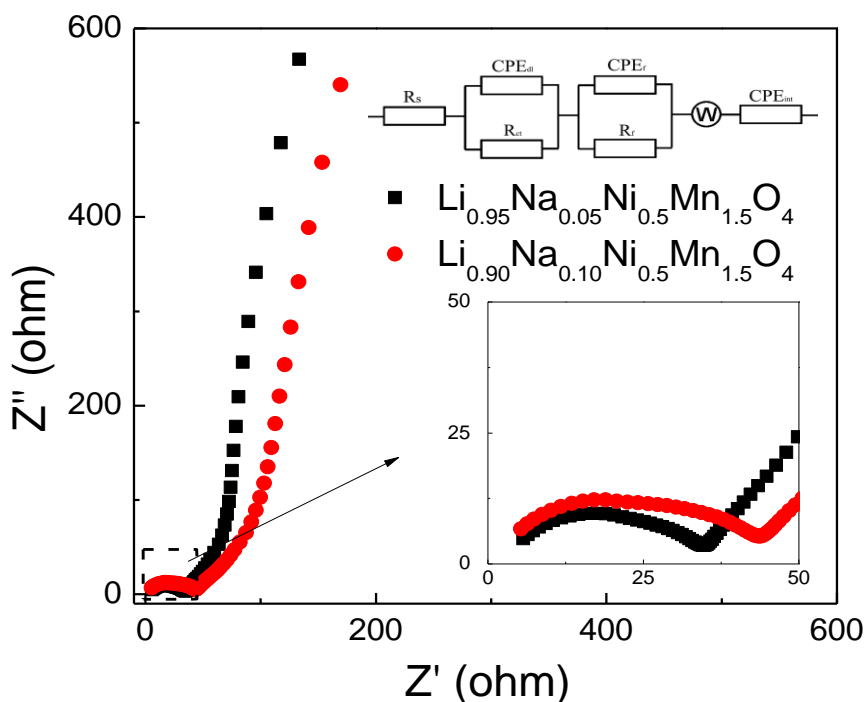


Figure 8. EIS spectra of $\text{Li}_{0.95}\text{Na}_{0.05}\text{Ni}_{0.5}\text{Mn}_{1.5}\text{O}_4$ and $\text{Li}_{0.90}\text{Na}_{0.10}\text{Ni}_{0.5}\text{Mn}_{1.5}\text{O}_4$ in the frequency range between 0.1 Hz and 100 kHz.

4. CONCLUSIONS

In this work, the $\text{Li}_{0.95}\text{Na}_{0.05}\text{Ni}_{0.5}\text{Mn}_{1.5}\text{O}_4$ and $\text{Li}_{0.90}\text{Na}_{0.10}\text{Ni}_{0.5}\text{Mn}_{1.5}\text{O}_4$ cathode materials were prepared by modified solution combustion synthesis method at 700°C . The two samples both deliver remarkable capacity retention approximately 91.0% after 500 cycles at 1C rate at 25°C . Meanwhile, the capacity retention of $\text{Li}_{0.95}\text{Na}_{0.05}\text{Ni}_{0.5}\text{Mn}_{1.5}\text{O}_4$ sample is 96.5% after 100 cycles at 10C rate, and can still deliver a specific capacity more than 110mAh/g, while the $\text{Li}_{0.90}\text{Na}_{0.10}\text{Ni}_{0.5}\text{Mn}_{1.5}\text{O}_4$ can only retain 91.4% at the same operation condition with a specific capacity of 95mAh/g.

ACKNOWLEDGEMENT

The authors gratefully acknowledge the financial supports from the National Natural Science Foundation of China (No. 51362012, No. 51662007 and U1602273), the Key Construction Disciplines of Chemistry for Master Degree Program in Yunnan, the Yunnan Local Colleges (part) Applied Basic Projects Joint Special Foundation (2017FH001-120) and the Yunnan Applied Basic Research Project (No.2017FD157).

References

1. B. Scrosati, *Nature*, 373 (1995) 557.

2. X. Li, W. Guo, Y. Liu, W. He and Z. Xiao, *Electrochim. Acta*, 116 (2014) 278.
3. Z.B. Ghassan, D.L. Rodolfo, C. Monica, and P. Guzay, *Renewable Sustainable Energy Rev.*, 89 (2018) 292.
4. F.W. Jeffrey, *J. Power Sources*, 195 (2010) 939.
5. J.L. Wang, Z.H. Li, J. Yang, J.J. Tang, J.J. Yu, W.B. Nie, G.T. Lei and Q.Z. Xiao, *Electrochim. Acta*, 75 (2012) 115.
6. D.Q. Liu, Y.H. Lu and J.B. Goodenough, *J. Electrochem. Soc.*, 157 (2010) A1269.
7. D.W. Shin, C.A. Bridges, A. Huq, M. P. Paranthaman and A. Manthiram, *Chem. Mater.*, 24 (2012) 3720.
8. T.F. Yi, Y. Xie, Y.R. Zhu, R.S. Zhu and M.F. Ye, *J. Power Sources*, 211 (2012) 59.
9. G.Y. Liu, H.Y. Sun, X. Kong, Y.N. Li and B.S. Wang, *INT. J. Electrochem. Sci.*, 10 (2015) 6651.
10. Z. Yang, Y. Jiang, J.H. Kim, Y. Wu, G.L. Li and Y.H. Huang, *Electrochim. Acta*, 117 (2014) 76.
11. E.S. Lee, K.W. Nam, E. Hu and A. Manthiram, *Chem. Mater.*, 24 (2012) 3610.
12. O. Sha, Z. Qiao, S.L. Wang, Z.Y. Tang, H. Wang, X.H. Zhang and Q. Xu, *Mater. Res. Bull.*, 48 (2013) 1606.
13. J.F. Wang, D. Chen, W. Wu, L. Wang and G.C. Liang, *Trans. Nonferrous Met. Soc. China*, 27 (2017) 2239.
14. J. Wang, W.Q. Lin, B.H. Wu and J.B. Zhao, *Electrochim. Acta*, 145 (2014) 245.
15. G.Y. Liu, X. Kong, H.Y. Sun and B.S. Wang, *Ceram. Int.*, 40 (2014) 14391.
16. H.Y. Sun, X. Kong, B.S. Wang, T.B. Luo and Guiyang Liu, *Int. J. Electrochem. Sci.*, 12 (2017) 8609
17. H.Y. Sun, X. Kong, B.S. Wang, T.B. Luo, Y. He and Guiyang Liu, *Int. J. Electrochem. Sci.*, 13 (2018) 4753.
18. H.Y. Sun, X. Kong, B.S. Wang, T.B. Luo and Guiyang Liu, *Ceram. Int.*, 44 (2018) 4603.
19. S. Patoux, L. Daniel, C. Bourbon, H. Lignier, C. Pagano, F.C. Le, S. Jouanneau and S. Martinet, *J. Power Sources* 189 (2009) 344.
20. G.B. Zhong, Y.Y. Wang, Z.C. Zhang and C.H. Chen, *Ceram. Int.*, 56 (2011) 6554.
21. F. Lantelme and E. Cherrat, *J. Electroanal. Chem. Interfacial Electrochem.*, 244 (1988) 61.
22. J.L. Wang, Z.H. Li, J. Yang, J.J. Tang, J.J. Yu, W.B. Nie, G.T. Lei and Q.Z. Xiao, *Electrochim. Acta*, 75 (2012) 115.
23. J. Liu and A. Manthiram, *Chem. Mater.*, 21 (2009) 1695.
24. A.Y. Shenouda and H.K. Liu, *J. Power Sources*, 185 (2008) 1386.
25. Q. Cao, H.P. Zhang, G.J. Wang, Q. Xia, Y.P. Wu and H.Q. Wu, *Electrochem. Commun.*, (2007) 1228.